TITLE:

In vivo dynamics of the cortical actin network revealed by fast-scanning atomic force microscopy

AUTHOR(S):

Zhang, Yanshu; Yoshida, Aiko; Sakai, Nobuaki; Uekusa, Yoshitsugu; Kumeta, Masahiro; Yoshimura, Shige H.

CITATION:

Zhang, Yanshu ...[et al]. In vivo dynamics of the cortical actin network revealed by fast-scanning atomic force microscopy. Microscopy 2017, 66(4): 272-282

ISSUE DATE:

2017-08

URL:

http://hdl.handle.net/2433/229445

RIGHT:

This is a pre-copyedited, author-produced PDF of an article accepted for publication in 'Microscopy' following peer review. The version of record 'Microscopy, Volume 66, Issue 4, 1 August 2017, Pages 272–282' is available online at: https://academic.oup.com/jmicro/article/66/4/272/3836920; The full-text file will be made open to the public on 20 May 2018 in accordance with publisher's 'Terms and Conditions for Self-Archiving'.; この論文は出版社版でありません。引用の際には出版社版をご確認ご利用ください。; This is not the published version. Please cite only the published version.

京都大学学術情報リポジトリ
KURENAI 紅
Kyoto University Research Information Repository

京都大学 KYOTO UNIVERSITY
A Self-archived copy in
Kyoto University Research Information Repository
https://repository.kulib.kyoto-u.ac.jp
京都大学学術情報リポジトリ KURENAI 紅 Kyoto University Research Information Repository

In vivo dynamics of the cortical actin network revealed by fast-scanning atomic force microscopy

Yanshu Zhang[1], Aiko Yoshida[1], Nobuaki Sakai[2], Yoshitsugu Uekusa[2], Masahiro Kumeta[1], and Shige H. Yoshimura[1]

[1]Graduate School of Biostudies, Kyoto University, Yoshida-konoe, Sakyo-ku, Kyoto 606-8501, Japan

[2]R&D Group, Olympus Corp., Tokyo 192-8512, Japan

Running title:

In vivo dynamics of cortical actin revealed by AFM

Keywords:

cortical actin, high-speed atomic force microscopy, actin-binding proteins, cell cortex, *in vivo* imaging, actin turnover

Corresponding Author:

Shige H. Yoshimura

Graduate School of Biostudies, Kyoto University

京都大学 KYOTO UNIVERSITY
A Self-archived copy in
Kyoto University Research Information Repository
https://repository.kulib.kyoto-u.ac.jp
京都大学学術情報リポジトリ KURENAI 紅 Kyoto University Research Information Repository

Yoshida-konoe, Sakyo-ku, Kyoto, 606-8501, Japan

tel&fax: +81-75-753-7906

e-mail: yoshimura@lif.kyoto-u.ac.jp

Authors' Information:

Yanshu Zhang: zhang.yanshu.58w@st.kyoto-u.ac.jp +81-75-753-7906

Aiko Yoshida: yoshida.aiko.46r@st.kyoto-u.ac.jp +81-75-753-7906

Nobuaki Sakai: no_sakai@ot.olympus.co.jp +81-42-691-8037

Yoshitsugu Uekusa: yoshitsugu1_uekusa@ot.olympus.co.jp +81-42-691-8037

Masahiro Kumeta: kumeta@lif.kyoto-u.ac.jp +81-75-753-7905

Shige H. Yoshimura: yoshimura@lif.kyoto-u.ac.jp +81-75-753-7906

京都大学 KYOTO UNIVERSITY
A Self-archived copy in
Kyoto University Research Information Repository
https://repository.kulib.kyoto-u.ac.jp
京都大学学術情報リポジトリ KURENAI 紅 Kyoto University Research Information Repository

Abstract

Together with lamellipodia and stress fibers, a dynamic network of actin filaments in the cell cortex plays a major role in the maintenance of cell morphology and motility. In contrast to lamellipodia, which have been well studied in various motile cells, the dynamics of actin filaments in the cell cortex have not yet been clarified due to a lack of proper imaging techniques. Here, we utilized high-speed atomic force microscopy for live-cell imaging and analyzed cortical actin dynamics in living cells. We successfully measured the polymerization rate and the frequency of filament synthesis in living COS-7 cells, and examined the associated effects of various inhibitors and actin-binding proteins. Actin filaments are synthesized beneath the plasma membrane and eventually descend into the cytoplasm. The inhibitors, cytochalasin B inhibited the polymerization, while jasplakinolide, inhibited the turnover of actin filaments as well as descension of the newly synthesized filaments, suggesting that actin polymerization near the membrane drives turnover of the cortical actin meshwork. We also determined how actin turnover is maintained and regulated by the free G-actin pool and G-actin binding proteins such as profilin and thymosin β4, and found that only a small amount of free G-actin was present in the cortex. Finally, we analyzed several different cell types, and found that the mesh size and the orientation of actin filaments were highly divergent, indicating the involvement of various actin-binding proteins in the maintenance and regulation of cortical actin architecture in each cell type.

京都大学 KYOTO UNIVERSITY
A Self-archived copy in
Kyoto University Research Information Repository
https://repository.kulib.kyoto-u.ac.jp
京都大学学術情報リポジトリ KURENAI 紅 Kyoto University Research Information Repository

Introduction

The cell cortex is a thin, dynamic architecture comprising the plasma membrane, actin, myosin, and a number of actin-associated proteins. Actin is a major cytoskeletal component of the cell cortex and plays critical roles in a number of events such as cell signaling, cell motility, and endocytosis [1]. Actin forms not only the cell cortex, but also other cellular architectures such as stress fibers, lamellipodium, and filopodium, each of which is regulated by different sets of proteins and plays a distinct role in cellular functions [2].

The dynamics of actin-based cellular architectures largely rely on the turnover of actin. Although actin monomers spontaneously form filaments *in vitro* [3, 4], a variety of proteins modify the dynamics, stability, and three-dimensional architectures of actin filaments in cells. For example, the Arp2/3 complex creates branched actin networks that are required for lamellipodia formation [5], whereas formins bind to the barbed end of actin filaments and are involved in the regulation and maintenance of proper actin network architecture and function [6]. Profilin, which binds to actin monomers, promotes actin assembly in the presence of cellular nucleation factors [7, 8]. Thymosin β4 is the main actin-sequestering protein in cells; it binds strongly to actin and prevents its assembly into filaments [1]. Fimbrin and α-actinin crosslink actin filaments to form a mesh-like network or thick bundles, whereas ADF/cofilin is actin-binding protein that severs the filament and increase depolymerization [9]. These regulatory proteins play different roles in different cellular architectures.

京都大学 KYOTO UNIVERSITY
A Self-archived copy in
Kyoto University Research Information Repository
https://repository.kulib.kyoto-u.ac.jp
京都大学学術情報リポジトリ KURENAI 紅 Kyoto University Research Information Repository

The spatial arrangement of actin filaments in the cortex has been studied by high-resolution techniques including electron microscopy [10]. A recent study using stochastic optical reconstruction microscopy revealed fine structural information on the network of actin filaments in the cell cortex [11]. However, in contrast to lamellipodia and other actin-related architectures, the dynamics of actin and its associated proteins in the cell cortex are poorly understood, mainly due to difficulties in resolving and visualizing these proteins by time-lapse fluorescence microscopy. Since the cortex is a dense network of randomly oriented actin filaments, it is difficult to visualize and resolve by conventional fluorescence microscopy, whereas stress fibers are thick bundles of actin and are easily visualized.

High-speed atomic force microscopy (HS-AFM) is an ideal tool for visualizing the dynamics of proteins and other biomolecules [12, 13]. So far, this technique already visualized various dynamic processes of importance in biological science for example myosin V walking on an actin filament [14], structural change of Ca^{2+}-pump [15] and rotary catalysis of F_1-ATPase [16]. HS-AFM was used for live cell imaging for the past few years. It enabled people to monitor the morphological changes of the bacterial cell surface [17]. Recent study succeeded in imaging larger objects such as live mammalian cells using a long-tip HS-AFM [18]. We previously used HS-AFM combined with inverted optical microscopy (BIXAM) to visualize the structural dynamics of the cell cortex including the plasma membrane [19, 20].

京都大学 KYOTO UNIVERSITY
A Self-archived copy in
Kyoto University Research Information Repository
https://repository.kulib.kyoto-u.ac.jp
京都大学学術情報リポジトリ KURENAI 紅 Kyoto University Research Information Repository

In this study, we used the same technique to visualize the dynamics of the cortical actin network and to analyze the polymerization/depolymerization process of cortical actin filaments in various cell types. In addition, we determined how actin turnover is maintained and regulated in living cells by actin-binding proteins, and affected by known inhibitors.

京都大学 KYOTO UNIVERSITY
A Self-archived copy in
Kyoto University Research Information Repository
https://repository.kulib.kyoto-u.ac.jp
京都大学学術情報リポジトリ KURENAI 紅 Kyoto University Research Information Repository

Methods

Cell culture and transfection

COS-7 cells, fibroblast-like cells derived from monkey kidney tissue, were grown on a poly-L-lysine-coated glass slide 1 or 2 days before AFM imaging at 37°C with 5% CO_2 in Dulbecco's Modified Eagle's Medium (DMEM) supplemented with 10% fetal bovine serum (FBS). AFM imaging was performed in DMEM supplemented with 10% FBS and 10 mM HEPES-NaOH (pH 7.0–7.6) (Sigma Aldrich, St. Louis, MO, USA). cDNA encoding human profilin-1 (Kazusa DNA clone #FXC06337) was cloned into pEGFP-C3 to create a fusion of profilin-1 with enhanced green fluorescent protein (EGFP). The mammalian expression vector for thymosin β4-mCherry was a kind gift from Dr. Harata (Tohoku University, Sendai, Japan). The plamids were introduced into cells using Effectene Transfection Reagent (Qiagen, Hilden, Germany) according to the manufacturer's protocol. At 24–48 h after transfection, the cells were used for AFM imaging. Expression of the fusion protein was confirmed by fluorescence signals from the cells.

AFM imaging and data analysis

BIXAM^{TM} (Olympus Corp., Tokyo, Japan), which is tip-scan type HS-AFM unit combined with an inverted fluorescent/optical microscope (IX83, Olympus) equipped with a phase-contrast system, was used for this study. The tip-scan HS-AFM imaging system was

京都大学 KYOTO UNIVERSITY
A Self-archived copy in
Kyoto University Research Information Repository
https://repository.kulib.kyoto-u.ac.jp
京都大学学術情報リポジトリ KURENAI 紅 Kyoto University Research Information Repository

developed based on a previous study [19, 20]. In brief, the modulation method was set to phase modulation mode to detect tip-sample interactions. An electron-beam deposited sharp cantilever tip with a spring constant of 0.1 N/m (USC-F0.8-k0.1, a customized cantilever from Nanoworld [Neuchâtel, Switzerland]) was used. The AFM tip was targeted to a specific area of the cell, based on phase-contrast or fluorescent imaging of the cell. The images were acquired at a scanning rate of 0.1 frames per second with a loading force less than 85 pN. It is determined by the equation:

$$F = \frac{a-b}{2} \times 100\ pN/nm, \quad (1)$$

where a, b are oscillation amplitudes before and after lowering the set point to apply a force to the cell's surface. The fluorescence signals were recorded with a charge-coupled device camera (DP71, Olympus) and an UPlan FLN objective lens (Olympus) at an excitation wavelength of 480 nm and an emission wavelength of 530 nm.

For image analysis, AFM images were exported as a series of Tag Image File Format files and analyzed using ImageJ (http://rsbweb.nih.gov/ij/) or MetaMorph (Molecular Device, Sunnyvale, CA, USA) software. The polymerization rate was calculated by chasing the distance between two filament ends in two consecutive AFM images. A curve was drawn to trace and calculate the elongation of actin filaments. The actin filament ends and movement were identified by 'invert' tool in ImageJ. The density and number of newly synthesized filamentous actin (F-actin) were calculated by extracting from 5 randomly selected areas of

京都大学 KYOTO UNIVERSITY
A Self-archived copy in
Kyoto University Research Information Repository
https://repository.kulib.kyoto-u.ac.jp
京都大学学術情報リポジトリ KURENAI 紅 Kyoto University Research Information Repository

$1\mu m^2$ in one frame of the AFM images. The vertical position was measured by drawing a horizontal line in randomly selected position on an actin filament and measured the intensity change of the same position in a succession of AFM images. For angular measurement, a horizontal line was treated as 0 degree, the angle below 90 degrees was measured.

Drug treatment

Cytochalasin B, CK-666, and SMIFH2 were purchased from Sigma, and jasplakinolide and blebbistatin were purchased from Abcam (Cambridge, UK). The reagents were added to the culture medium at final concentrations of 2 μM cytochalasin B, 50 μM CK-666, 10.6 μM SMIFH2, 1 μM Jasplakinolide, and 50 μM blebbistatin.

京都大学 KYOTO UNIVERSITY
A Self-archived copy in
Kyoto University Research Information Repository
https://repository.kulib.kyoto-u.ac.jp
京都大学学術情報リポジトリ KURENAI 紅 Kyoto University Research Information Repository

Results

Actin turnover in the cortical layer

The cortical actin layer in living COS-7 cells was visualized by BIXAM. The time-lapse observation of the cell cortex revealed dynamic rearrangement of the actin network including polymerization/depolymerization of individual filaments (Fig. 1, Supplementary Video 1). Subtraction of two consecutive frame images clearly allowed visualization of the new filaments and the disappeared convergent actin structures (Fig. 1 b). The average formation rate of new filaments was 0.19 ± 0.08 $\mu m^{-2}sec^{-1}$, most of which appeared within a single frame (10 s) during the observation. However, elongation of the end of the filament was occasionally observed in several frames (Fig. 1 c, for more details, see Supplementary Fig. S1), at an elongation rate of 0.19 ± 0.07 μm/sec (~11.4 μm/min). To determine whether this elongation was due to the sliding of F-actin or actin polymerization at the end of the filament, cells were treated with cytochalasin B, an inhibitor of actin polymerization [21] or blebbistatin, an inhibitor of non-muscle myosin II [22]. As summarized in Figure 1 d and 1 e (also see Supplementary Videos 2 and 3), elongation at the end of the filament was inhibited by cytochalasin B, but not by blebbistatin, indicating that filament elongation was due to F-actin polymerization at the barbed end. The observed polymerization rate (0.19 μm/sec) corresponded to 70 G-actin/sec. Also, to determine whether the new appeared actin filaments are newly synthesized actin filaments, we compared the number of appeared actin filament

京都大学 KYOTO UNIVERSITY
A Self-archived copy in
Kyoto University Research Information Repository
https://repository.kulib.kyoto-u.ac.jp
京都大学学術情報リポジトリ KURENAI 紅 Kyoto University Research Information Repository

before and after the treatment of cytochalasin B, and found that the number of new appeared actin filaments significantly decreased after the treatment of cytochalasin B (Fig. 1 e). It indicates that the appeared actin filaments are the newly synthesized actin filaments (see Discussion section).

Descension of newly synthesized filaments into the cytoplasm

We examined the fate of newly synthesized actin filaments in the cell cortex (Fig. 2). Analysis of the actin filaments revealed that polymerization mainly occurred near the plasma membrane, and that the newly synthesized filament gradually descended into the interior of the cell (Fig. 2 a). Statistical analyses from more than 20 filaments revealed that most of them descended downwards into the interior of the cell and eventually disappeared 10–90 s after synthesis. These observations suggest that actin polymerization occurs near the plasma membrane, possibly mediated by various membrane-bound proteins (see Discussion section).

The spatial and time resolutions of our AFM setup did not allow us to determine if filament disappearance was due to descension outside the imaging depth or depolymerization occurring in the middle of descension. In contrast to the polymerizing end, the depolymerizing end was rarely captured in our time-lapse images. Considering the dissociation rate constants of F-actin (0.89 s^{-1} and 0.19 s^{-1} for the barbed and pointed ends, respectively [23]), it has been speculated that most newly synthesized filaments descend

京都大学 KYOTO UNIVERSITY
A Self-archived copy in
Kyoto University Research Information Repository
https://repository.kulib.kyoto-u.ac.jp
京都大学学術情報リポジトリ KURENAI 紅 Kyoto University Research Information Repository

outside the imaging depth before they are completely depolymerized. This is in accordance with the fact that the actin filament density determined by AFM (10.02 ± 0.63 μm^{-2}) is less than that determined by image-based photometry [24].

Inhibition of polymerization/depolymerization turnover

We elucidated how cortical actin dynamics (e.g., polymerization rate, frequency of new filament synthesis, descension of filaments) are affected by inhibitors. Jasplakinolide is a small cyclic peptide that was isolated from the marine sponge, *Jaspis johnstoni*, and inhibits actin depolymerization [25]. Interestingly, the addition of jasplakinolide (1 μM) to COS-7 cells immediately reduced not only depolymerization but also polymerization frequencies without changing the filament density over time (Fig. 3, Supplementary Videos 4). The AFM image revealed that new filament synthesis was rarely observed (~0.02 $\mu m^{-2}sec^{-1}$) (Fig. 3 b). Based on several observations of polymerization, the polymerization rate was calculated as 0.13 ± 0.04 μm/sec (Fig. 3 d). The fact that inhibition of depolymerization immediately reduced the polymerization rate indicates that a small amount of free G-actin was present in the cell cortex, which was rapidly depleted by inhibition of depolymerization (see Discussion section). Notably, jasplakinolide also inhibited descension of the filament network into the cytoplasm (Fig. 3 e), suggesting that descension into the cortical layer is driven by actin filament synthesis near the plasma membrane.

京都大学 KYOTO UNIVERSITY
A Self-archived copy in
Kyoto University Research Information Repository
https://repository.kulib.kyoto-u.ac.jp
京都大学学術情報リポジトリ KURENAI 紅 Kyoto University Research Information Repository

Maintenance of the free G-actin pool in the cell cortex

The polymerization/depolymerization turnover of intracellular actin is one of the important issues in the regulation of actin. Therefore, we examined the effects of actin-binding proteins to characterize the intracellular pool of G-actin in COS-7 cells.

To estimate the amount of the free G-actin pool, we overexpressed several actin-binding proteins that regulate actin turnover. Profilin binds to G-actin and regulates actin polymerization, whereas thymosin β4 competes with profilin binding to G-actin and sequesters actin monomers from forming actin filaments [1]. We overexpressed EGFP-profilin and mCherry-thymosin β4 in COS-7 cells, and examined the dynamics of polymerization/depolymerization. The analysis of cortical actin filaments in the overexpressing cells revealed that these proteins had little effects on polymerization rate and density (Fig. 4, Supplementary Videos 5 and 6), indicating that these proteins are either not involved in actin turnover or that the cytoplasmic G-actin pool is already saturated by endogenous amounts of profilin and thymosin β4.

We also examined the involvement of other actin regulatory proteins in the maintenance of cortical actin. Arp2/3 complex and formins are involved in the maintenance and regulation of actin architectures, particularly in the lamellipodium and contractile ring [2]. However, inhibitors of Arp2/3 and formins (CK666 and SMIFH2, respectively) did not affect

京都大学 KYOTO UNIVERSITY
A Self-archived copy in
Kyoto University Research Information Repository
https://repository.kulib.kyoto-u.ac.jp
京都大学学術情報リポジトリ KURENAI 紅 Kyoto University Research Information Repository

actin density, the amount of newly synthesized F-actin, or the polymerization rate in the cortex (Supplementary Fig. S2). These results indicate that formins and the Arp2/3 complex are not involved in the steady-state dynamics of cortical actin.

Cell type-specific arrangement and dynamics of the cortical actin network

The structure and dynamics of the cortical actin network were analyzed and compared in different cell types. In addition to COS-7 cells, NIH-3T3 mouse embryonic fibroblast cells, C2C12 mouse myoblast cells, ST2 mouse bone marrow-derived stromal cells, and XTC frog fibroblast cells were imaged and analyzed (Fig. 5, Supplementary Videos 7–10). As summarized in Figure 5 a, the arrangement of actin filaments was highly divergent in different cell types. The actin filaments of NIH-3T3 cells appeared to be bundled and did not form an actin mesh (Fig. 5 a). The polymerization rate was not significantly different among cell types (Fig 5 b). On the other hand, there was large variance in the turnover rate (Fig. 5 c); the number of newly synthesized F-actin was high in ST2 (0.19 $\mu m^{-2}sec^{-1}$) and C2C12 (0.24 $\mu m^{-2}sec^{-1}$) cells, and was lowest (0.10 $\mu m^{-2}sec^{-1}$) in XTC cells. The mesh size of actin in ST2, C2C12, and XTC cells also largely varied; C2C12 had the most dense (smallest mesh size) network and XTC had the largest mesh size (Fig. 5 d). The orientation of actin filaments was random in COS-7, XTC, and undifferentiated C2C12 and ST2 cells, whereas in NIH-3T3 cells, actin was oriented to the longer axis of the cell (Fig. 5 e). These results suggest that the

京都大学 KYOTO UNIVERSITY
A Self-archived copy in
Kyoto University Research Information Repository
https://repository.kulib.kyoto-u.ac.jp
京都大学学術情報リポジトリ KURENAI 紅 Kyoto University Research Information Repository

initiation step was regulated by different mechanisms, but the elongation step proceeded by a similar mechanism in the examined cell lines.

Discussion

In this study, we successfully visualized the dynamics of the cortical actin network in living COS-7 cells, and revealed the effects of actin-binding proteins and inhibitors. Analysis of the steady-state dynamics of cortical actin filaments in living cells has been difficult to accomplish due to a lack of live-cell imaging techniques with high spatiotemporal resolution. The HS-AFM, which was specially designed for live-cell imaging, allowed visualization of a single actin filament in the cell cortex without any staining and labeling. Thus, our approach presented here provides a novel method for analyzing the turnover of intracellular actin and the role of actin-associated proteins.

Actin polymerization rates in vitro and in the cell cortex

We observed the polymerization process on the barbed end of F-actin in the cortex of living COS-7 cells (Fig. 1). Cytochalasin B, which inhibits actin monomers from being added to the barbed end of filaments [16], significantly reduced the rate of polymerization (Fig. 1 d). In the maximum scanning area of our AFM setup (4.5 x 6 μm^2, 640 x 480 pixels), most of the newly synthesized filaments appeared within a single frame (10 sec). Occasionally, barbed-end

京都大学 KYOTO UNIVERSITY
A Self-archived copy in
Kyoto University Research Information Repository
https://repository.kulib.kyoto-u.ac.jp
京都大学学術情報リポジトリ KURENAI 紅 Kyoto University Research Information Repository

filament elongation was captured in several frames (Fig. 1) at an average rate of 0.19 μm/sec.

The polymerization rate of actin has been extensively studied in *in vitro* experiments. The rate constant at the barbed end in solution was 11.6 $\mu M^{-1}sec^{-1}$ [26]. The time-lapse observation of fluorescently labeled actin by total internal reflection fluorescence microscope provided a similar value (~10 $\mu M^{-1}sec^{-1}$) [27]. The polymerization rate that we chased in the series of AFM images (0.19 μm/sec) corresponded to ~70 subunits per second. If we excluded the involvement of actin regulatory proteins in the polymerization process, the observed rate was 6.3–7.3 μM of free actin in the cortex. This is much lower than the value reported by biochemical approaches (~30 μM [28]), but is in accordance with our own observations that the cell cortex contains very low amounts of free actin (Fig. 3 and Fig. 4).

Cortical actin layer is descending by newly-synthesized filaments at the plasma membrane

We found that the filaments were newly synthesized near the plasma membrane and gradually descended into the interior of the cell (Fig. 2). We never observed the filaments ascending towards the plasma membrane. These results indicate that polymerization always occurs at the inner surface of the plasma membrane. A previous study has shown that membrane phosphoinositide lipids can associate with several actin-binding proteins and regulate their activities [29]. Our results also suggest involvement of the plasma membrane and its associated proteins for the initiation of polymerization. Addition of jasplakinolide not only

京都大学 KYOTO UNIVERSITY
A Self-archived copy in
Kyoto University Research Information Repository
https://repository.kulib.kyoto-u.ac.jp
京都大学学術情報リポジトリ KURENAI 紅 Kyoto University Research Information Repository

inhibited polymerization/depolymerization turnover of cortical actin but also the descending movement of the filaments (Fig. 3). These results clearly demonstrate that descension of the filament within the cortical layer is driven by new filament synthesis near the plasma membrane.

At the end of the cortical layer, the filaments should be depolymerized. This process might be actively catalyzed by severing proteins, such as cofilin (as is the case in lamellipodia) or by spontaneous depolymerization. When the half-life ($t_{1/2}$) of cortical actin (20–30 s) obtained by fluorescence recovery after photobleaching (FRAP) analysis [30] and the dissociation rate constant obtained *in vitro* (0.89 s^{-1} and 0.19 s^{-1} for barbed and pointed ends, respectively) are considered, it can be speculated that the active severing of filaments might be occurred during the descension. Although the biological significance of filament descension in the cortical layer is still not understood, it is possible that it may play a role in driving endocytic vesicles into the cytoplasm.

How the actin monomer pool is maintained

Measuring the amount of free actin is important because the turnover dynamics of cellular actin depends upon the amount of free G-actin and F-actin, as well as the function number of regulatory proteins. The immediate decrease in depolymerization and polymerization upon treatment with jasplakinolide (Fig. 3) suggests that only a small amount of free G-actin is

京都大学 KYOTO UNIVERSITY
A Self-archived copy in
Kyoto University Research Information Repository
https://repository.kulib.kyoto-u.ac.jp
京都大学学術情報リポジトリ KURENAI 紅 Kyoto University Research Information Repository

present in the cortex. The density of the filament remained constant after addition of the inhibitor (Fig. 3 c), indicating that free G actin in the cytoplasm, or at least in the cortical layer of COS-7 cells is maintained at very low levels. The estimation of free G-actin concentration from the observed polymerization rate (0.19 μm/sec) was 6–7 μM, which is lower than that previously estimated by biochemical fractionation (30 μM [28]). This might be because biochemical quantification does not measure the local amount of G-actin within the cell; thus, a large free G-actin pool may exist in the cytoplasm, while the pool in the cell cortex is small. Alternatively, a large amount of G-actin exists in cells, but most are sequestered by thymosin β4, and as such, cannot be directly involved in polymerization. The latter possibility aligns well with the previous report that the intracellular amount of thymosin β4 is comparable to that of actin (100–500 μM) [31], and also with the results of our experiment, in which the overexpression of profilin or thymosin β4 did not affect the turnover dynamics of cortical actin filaments (Fig. 4), which is consistent with the previous study supports that although little effects were observed in cell cortex, thymosin β4 may play a role in building protrusions in cell invasion or wound repair by influencing the strength and force produced by actin [32].

There are a number of proteins that regulate the cellular dynamics of actin turnover such as those that bind actin monomers (profilin, thymosin β4) and those that bind the filament (cofilin, capping protein, Arp2/3 complex), all of which cooperate to maintain the

京都大学 KYOTO UNIVERSITY
A Self-archived copy in
Kyoto University Research Information Repository
https://repository.kulib.kyoto-u.ac.jp
京都大学学術情報リポジトリ KURENAI 紅 Kyoto University Research Information Repository

pool of free unpolymerized actin. Profilin binds to actin monomers and inhibits spontaneous nucleation. It also stimulates the elongation of barbed ends in the presence of formin. The intracellular profilin concentration (10–80 μM [33]) is comparable to that of actin; profilin are supposed to bind to the entire pool of unpolymerized actin monomers in amoeba cells [34]. Thymosin β4 also binds to ATP-actin monomers and blocks all actin assembly reactions including nucleation and growth at both ends. It competes with profilin for binding actin, but profilin binds actin monomers more tightly than thymosin β4, which allows profilin to maintain a pool of actin that is ready to elongate barbed ends, while thymosin β4 holds the rest of the monomers in reserve. Together with these reports, our results described in Figures 3 and 4 suggest that at least two endogenous actin buffering systems (profilin and thymosin β4) maintain the free actin pool in the cell cortex at low levels.

Different regulatory mechanism in the cortex and lamellipodia

It is intriguing that proteins involved in maintenance of the actin network in lamellipodia (formins and Arp2/3 complex) do not play a role in the cortex (Supplementary Fig. S2). Formins are involved in formation of the actin network in cell division, migration, adhesion, membrane blebbing [28, 35], and is also involved in formation of the contractile ring in yeast [36]. FRAP analysis of melanoma cells demonstrated that SMIFH2, a formin inhibitor, affected the turnover rate of cortical actin [10]. However, our observations in COS-7 cells by

京都大学 KYOTO UNIVERSITY
A Self-archived copy in
Kyoto University Research Information Repository
https://repository.kulib.kyoto-u.ac.jp
京都大学学術情報リポジトリ KURENAI 紅 Kyoto University Research Information Repository

AFM revealed that SMIFH2 did not affect the polymerization rate, synthesis of F-actin, or density of the filaments (Supplementary Fig. S2). These results indicate that formins are not actively involved in the steady-state polymerization of cortical actin, but may play a role in other active processes such as re-organization of the actin network in mitosis.

Similar results were obtained using CK666, an inhibitor of the Arp2/3 complex. The Arp2/3 complex binds to F-actin and generates a branching point on the filament. It promotes actin nucleation at a 70° branch angle to the parent filament and plays critical roles in formation of the actin network at the leading edge of motile cells [37–39], formation of the contractile ring [36], and wound healing in the cell cortex [40]. On the other hand, our AFM observation of the cell cortex revealed that inhibition of the Arp2/3 complex did not affect the polymerization rate and density of actin (Supplementary Fig. S2).

There are a number of barbed ends in the lamellipodium due to Arp2/3-mediated branching. Although some of the barbed ends are capped by capping proteins, a number of free barbed ends elongate towards the plasma membrane, which generates a mechanical force against the plasma membrane and pushes the cell edge outward. In contrast, cortical actin filament polymerizes mainly in the direction parallel to the plasma membrane. Our results suggest that the branching activity of Arp2/3 complex might be very low in the cortex, possibly due to the absence of activating proteins such as Neural Wiskott-Aldrich Syndrome Protein. The mechanism underlying the synthesis of actin filament near the plasma membrane

京都大学 KYOTO UNIVERSITY
A Self-archived copy in
Kyoto University Research Information Repository
https://repository.kulib.kyoto-u.ac.jp
京都大学学術情報リポジトリ KURENAI 紅 Kyoto University Research Information Repository

has not yet been clarified. It is possible that ezrin/radixin/moesin (ERM) complex, which associates the plasma membrane and also binds to actin [41], might be involved in the nucleation of actin in the cell cortex.

Cell type-specific organization of actin network

The AFM observation of cortical actin in different cell types revealed that structural cortical networks differed in these cells (Fig. 5). NIH-3T3 fibroblasts have bundles of actin filaments, whereas the other cell lines (COS-7, ST2, C2C12, and XTC) have mesh-like network of filaments. Analysis of the filament angle (Fig. 5 e) demonstrated that filaments are oriented to the longer cell axis in NIH-3T3 cells.

Cells use the actomyosin structure to cause stress, which triggers changes in shape changing and responses to stimuli. For example, platelets generate isotropic contractions to reduce their size while fibroblasts generate anisotropic stress [42]. Thus, the different orientations and mesh sizes of actin filaments generate different types of contractions to modulate the cell shape and response to the stimuli.

Concluding Remarks

In this study, we described a new approach for analyzing cortical actin dynamics in living cells, as well as its related processes. Our results indicate that in the cell cortex, actin

京都大学 KYOTO UNIVERSITY
A Self-archived copy in
Kyoto University Research Information Repository
https://repository.kulib.kyoto-u.ac.jp
京都大学学術情報リポジトリ KURENAI 紅 Kyoto University Research Information Repository

polymerization occurs mainly on the inner surface of the plasma membrane in an Arp2/3- and formin-independent manner, and the synthesized filaments gradually descend down into the interior of the cytoplasm where it is depolymerized to maintain a constant G-actin pool. Although we visualized the polymerization events in live cells, higher temporal resolution is still needed to track these events in their entirety. In addition, many questions still remain unanswered, for example, how new barbed ends are created in the cell cortex, how actin turnover is regulated, and how free G-actin actin pool is maintained and distributed in the cortex. These are important questions for clarifying the structural function dynamics of the cell cortex.

Acknowledgments

The mammalian expression vector for thymosin β4 was a kind gift from Dr. Hrata from Tohoku University (Sendai, Japan). The XTC cells were a kind gift from Dr. Watanabe from Kyoto University (Kyoto, Japan). This work was supported by the Grant-in-Aid for Challenging Exploratory Research (No. 16K14722 to S.H.Y), the Grant-in-Aid for Young Scientists (No. 26870302 to M.K.) from the Japan Society for the Promotion of Science (JSPS), and the Advanced Research & Development Programs for Medical Innovation from the Japan Agency for Medical Research and Development (No. 16gm5810018h0001 to SHY). A.Y. is a recipient of the JSPS research fellow. We would also like to thank Mr. Ito, Mr. Yagi and Ms. Imaoka for their technical assistance.

京都大学
KYOTO UNIVERSITY
A Self-archived copy in
Kyoto University Research Information Repository
https://repository.kulib.kyoto-u.ac.jp
京都大学学術情報リポジトリ
KURENAI 紅
Kyoto University Research Information Repository

京都大学 KYOTO UNIVERSITY
A Self-archived copy in
Kyoto University Research Information Repository
https://repository.kulib.kyoto-u.ac.jp
京都大学学術情報リポジトリ KURENAI 紅 Kyoto University Research Information Repository

References

[1] Alberts B, Johnson A, Lewis J, Morgan D, Raff M, Roberts K, and Walter P (2015) *Molecular Biology of The Cell Sixth Edition*. (Taylor&Francis Group, New York.)

[2] Blanchoin L, Boujemaa-Paterski R, Sykes C, and Plastino J (2014) Actin dynamics, architecture, and mechanics in cell motility. *Physiol. Rev.* **94**, 235-263.

[3] Pollard T D, and Mooseker M S (1981) Direct measurement of actin polymerization rate constants by electron-microscopy of actin-filaments nucleated by isolated microvillus cores. *J. Cell Biol.* **88**, 654–659.

[4] Doolittle L K, Rosen M K, and Padrick S B (2013) Measurement and analysis of *in vitro* actin polymerization. *Methods Mol. Biol.* **1046**, 273–293.

[5] Svitkina T M, and Borisy G G (1999) Arp2/3 complex and actin depolymerizing factor/cofilin in dendritic organization and treadmilling of actin filament array in lamellipodia. *J. Cell Biol.* **145**, 1009–1026.

[6] Pruyne D, Evangelista M, Yang C, Bi E, Zigmond S, Bretscher A, and Boone C (2002) Role of formins in actin assembly: nucleation and barbed-end association. *Science* **297**, 612–615.

[7] Kovar D R, Harris E S, Mahaffy R, Higgs H N, and Pollard T D (2006) Control of the assembly of ATP- and ADP-actin by formins and profilin. *Cell* **124**, 423–435.

京都大学 KYOTO UNIVERSITY
A Self-archived copy in
Kyoto University Research Information Repository
https://repository.kulib.kyoto-u.ac.jp
京都大学学術情報リポジトリ KURENAI 紅 Kyoto University Research Information Repository

[8] Chereau D, Kerff F, Graceffa P, Grabarek Z, Langsetmo K, and Dominguez R (2005) Actin-bound structures of Wiskott-Aldrich syndrome protein (WASP)-homology domain 2 and the implications for filament assembly. *Proc. Natl. Acad. Sci. U. S. A.* **102**, 16644–16649.

[9] Reymann A C, Suarez C, Guérin C, Martiel J L, Staiger C J, Blanchoin L, and Boujemaa-Paterski R (2011) Turnover of branched actin filament networks by stochastic fragmentation with ADF/cofilin. *Mol. Biol. Cell* **22**, 2541–2550.

[10] Morone N, Fujiwara T, Murase K, Kasai R S, Ike H, Yuasa S, Usukura J, and Kusumi A (2006) Three-dimensional reconstruction of the membrane skeleton at the plasma membrane interface by electron tomography. *J. Cell Biol.* **174**, 851–862.

[11] Xu K, Babcock H P, and Zhuang X (2012) Dual-objective STORM reveals three-dimensional filament organization in the actin cytoskeleton. *Nat. Methods* **9**, 185–188.

[12] Yokokawa M, Wada C, Ando T, Sakai N, Yagi A, Yoshimura S H, and Takeyasu K (2006) Fast-scanning atomic force microscopy reveals the ATP/ADP-dependent conformational changes of GroEL. *EMBO J.* **25**, 4567–4576.

[13] Gilmore J L, Suzuki Y, Tamulaitis G, Siksnys V, Takeyasu K, and Lyubchenko Y L (2009) Single-molecule dynamics of the DNA-EcoRII protein complexes revealed with high-speed atomic force microscopy. *Biochemistry* **48**, 10492–10498.

京都大学 KYOTO UNIVERSITY
A Self-archived copy in
Kyoto University Research Information Repository
https://repository.kulib.kyoto-u.ac.jp
京都大学学術情報リポジトリ KURENAI 紅 Kyoto University Research Information Repository

[14] Kodera N, Yamamoto D, Ishikawa R, and Ando T (2010) Video imaging of walking myosin V by high-speed atomic force microscopy. *Nature*, **468**, 72–76.

[15] Yokokawa M, and Takeyasu K (2011) Motion of the Ca^{2+}-pump captured. *FEBS J.* **278**, 3025–3031.

[16] Uchihashi T, Iino R, Ando T, and Noji H (2011) High-speed atomic force microscopy reveals rotary catalysis of rotorless F_1-ATPase. *Science*, **333**, 755.

[17] Uchihashi T, Watanabe H, Fukuda S, Shibata M, Ando T (2016) Functional extension of high-speed AFM for wider biological applications. *Ultramicroscopy*, **160**, 182–196.

[18] Shibata M, Uchihashi T, Ando T, and Yasuda R (2015) Long-tip high-speed atomic force microscopy for nanometer-scale imaging in live cells. *Sci. Rep*, **5**, 8724.

[19] Suzuki Y, Sakai N, Yoshida A, Uekusa Y, Yagi A, Imaoka Y, Ito S, Karaki K, and Takeyasu K (2013) High-speed atomic force microscopy combined with inverted optical microscopy for studying cellular events. *Sci. Rep.* **3**, 2131.

[20] Yoshida A, Sakai N, Uekusa Y, Deguchi K, Gilmore J L, Kumeta M, Ito S, and Takeyasu K (2015) Probing in vivo dynamics of mitochondria and cortical actin networks using high-speed atomic force/fluorescence microscopy. *Genes to Cells* **20**, 85–94.

[21] MacLean-Fletcher S, and Pollard T D (1980) Mechanism of action of cytochalasin B on actin. *Cell* **20**, 329–341.

京都大学 KYOTO UNIVERSITY
A Self-archived copy in
Kyoto University Research Information Repository
https://repository.kulib.kyoto-u.ac.jp
京都大学学術情報リポジトリ KURENAI 紅 Kyoto University Research Information Repository

[22] Limouze J, Straight A F, Mitchison T, and Sellers J R (2004) Specificity of blebbistatin, an inhibitor of myosin II. *J. Muscle Res. Cell Motil.* **25**, 337–341.

[23] Kuhn J R, and Pollard T D (2005) Real-time measurements of actin filament polymerization by total internal reflection fluorescence microscopy. *Biophys. J.* **88**, 1387–1402.

[24] Abraham V C, Krishnamurthi V, Taylor D L, and Lanni F (1999) The actin-based nanomachine at the leading edge of migrating cells. *Biophys. J.* **77**, 1721–1732.

[25] Bubb M R, Spector I, Beyer B B, and Fosen K M (2000) Effect of Jasplakinolide on the kinetics of actin polymerization. *Biochemistry* **275**, 5163–5170.

[26] Pollard T D (1986) Rate constants for the reactions of ATP-and ADP-actin with the ends of actin filaments. *J. Cell Biol.* **103**, 2747.

[27] Fujiwara I, Takahashi S, Tadakuma H, Funatsu T, and Ishiwata S (2002) Microscopic analysis of polymerization dynamics with individual actin filaments. *Nat. Cell Biol.* **4**, 666–673.

[28] Goode B L, and Eck M J (2007) Mechanism and function of formins in the control of actin assembly. *Annu. Rev. Biochem.* **76**, 593–627.

[29] Bezanilla M, Gladfelter A S, Kovar D R, and Lee W (2015) Cytoskeletal dynamics: A view from the membrane. *J. Cell Biol.* **209**, 329–337.

京都大学 KYOTO UNIVERSITY
A Self-archived copy in
Kyoto University Research Information Repository
https://repository.kulib.kyoto-u.ac.jp
京都大学学術情報リポジトリ KURENAI 紅 Kyoto University Research Information Repository

[30] Fritzsche M, Lewalle A, Duke T, Kruse K, and Charras G (2013) Analysis of turnover dynamics of the submembranous actin cortex. *Mol. Biol. Cell* **24**, 757–767.

[31] Xue B, Leyrat C, Grimes J M, and Robinson R C (2014) Structural basis of thymosin-β4/profilin exchange leading to actin filament polymerization. *Proc. Natl. Acad. Sci. U. S. A.* **111**, E4596-4605.

[32] Carlier M F, Hertzog M, Didry D, Renault L, Cantrelle F X, Heijenoort C V, Knossow M, and Guittet E (2007) Structure, function, and evolution of the β-thymosin/WH2 (WASP-homology2) actin-binding module. *Ann. N. Y. Acad. Sci.*, **1112**, 67–75.

[33] Pernier J, Shekhar S, Jegou A, Guichard B, and Carlier M F (2016) Profilin interaction with actin filament barbed end controls dynamic instability, capping, branching, and motility. *Dev. Cell* **36**, 201–214.

[34] Vinson V K, De La Cruz E M, Higgs H N, and Pollard T D (1998) Interactions of acanthamoeba profilin with actin and nucleotides bound to actin. *Biochemistry* **37**, 10871–10880.

[35] Bovellan M, Romeo Y, Biro M, Boden A, Chugh P, Yonis A, Vaghela M, Fritzsche M, Moulding D, Thorogate R, Jegou A, Thrasher A J, Romet-Lemonne G, Roux P P, Paluch E K, and Charras G (2014) Cellular control of cortical actin nucleation. *Curr. Biol.* **24**, 1628–1635.

[36] Pelham R J, and Chang F (2002) Actin dynamics in the contractile ring during cytokinesis in fission yeast. *Nature* **419**, 82–86.

京都大学 KYOTO UNIVERSITY
A Self-archived copy in
Kyoto University Research Information Repository
https://repository.kulib.kyoto-u.ac.jp
京都大学学術情報リポジトリ KURENAI 紅 Kyoto University Research Information Repository

[37] Welch M D, DePace A H, Verma S, Iwamatsu A, and Mitchison T J (1997) The human Arp2/3 complex is composed of evolutionarily conserved subunits and is localized to cellular regions of dynamic actin filament assembly. *J. Cell Biol.* **138**, 375–384.

[38] Lai F P, Szczodrak M, Block J, Faix J, Breitsprecher D, Mannherz H G, Stradal T E, Dunn G A, Small J V, and Rottner K (2008) Arp2/3 complex interactions and actin network turnover in lamellipodia. *EMBO J.* **27**, 982–992.

[39] Yang Q, Zhang X F, Pollard T D, and Forscher P (2012) Arp2/3 complex-dependent actin networks constrain myosin II function in driving retrograde actin flow. *J. Cell Biol.* **197**, 939–956.

[40] Vinzenz M, Nemethova M, Schur F, Mueller J, Narita A, Urban E, Winkler C, Schmeiser C, Koestler S A, Rottner K, Guenter P R, Maeda Y, and Small J V (2012) Actin branching in the initiation and maintenance of lamellipodia. *J. Cell Sci.* **125**, 2775–2785.

[41] Ivetic A, and Ridley A J (2004) Ezrin/radixin/moesin proteins and Rho GTPase signaling in leucocytes. *Immunology* **112**, 165–176.

[42] Murrell M, Oakes P W, Lenz M, and Gardel M L (2015) Forcing cells into shape: the mechanics of actomyosin contractility. *Mol. Cell Boil.* **16**, 486–498.

京都大学 KYOTO UNIVERSITY
A Self-archived copy in
Kyoto University Research Information Repository
https://repository.kulib.kyoto-u.ac.jp
京都大学学術情報リポジトリ KURENAI 紅 Kyoto University Research Information Repository

Figure Legends

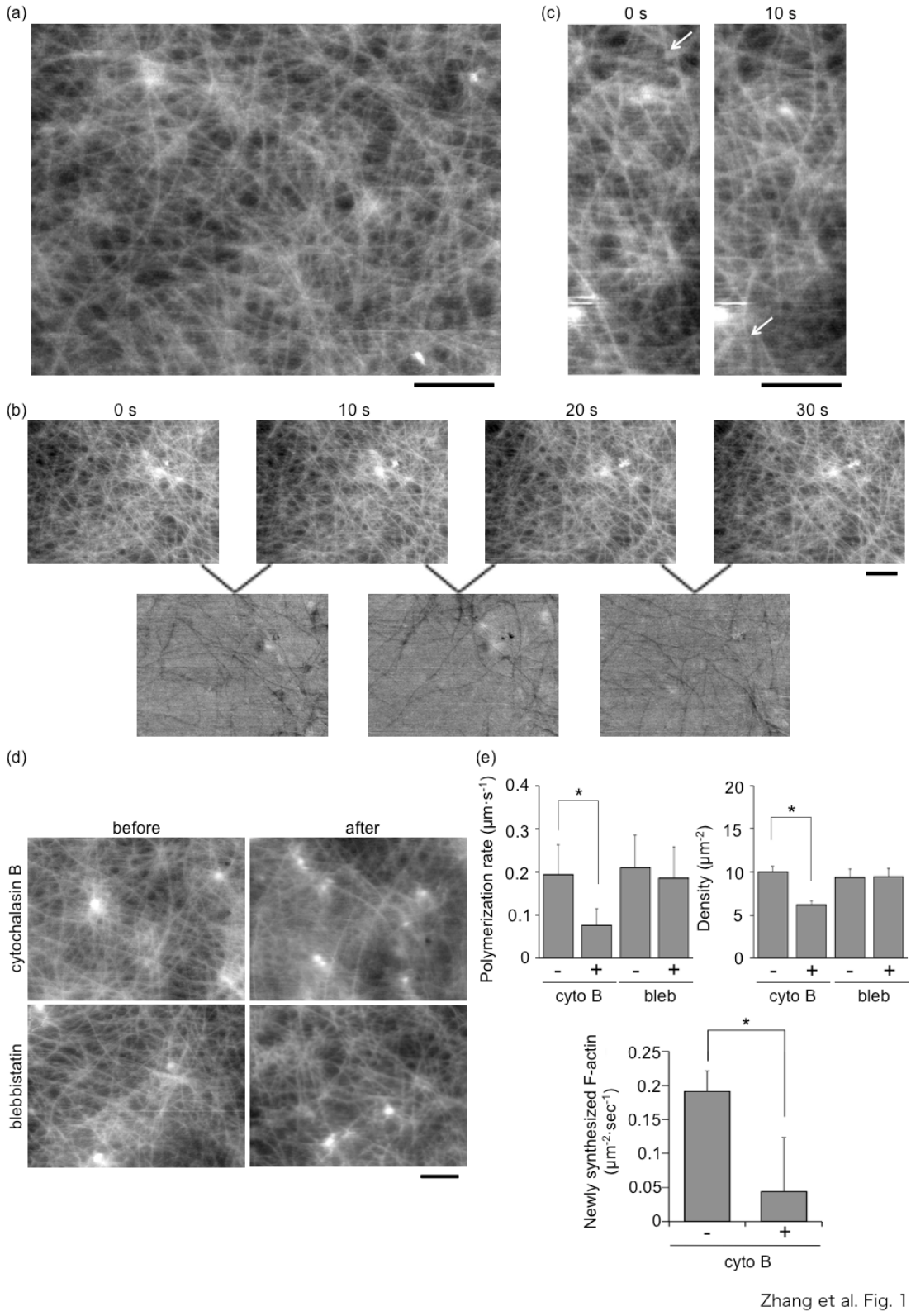

Fig. 1. Dynamics of the cortical actin layer in COS-7 cells. (a) Snapshot AFM image of

京都大学 KYOTO UNIVERSITY
A Self-archived copy in
Kyoto University Research Information Repository
https://repository.kulib.kyoto-u.ac.jp
京都大学学術情報リポジトリ KURENAI 紅 Kyoto University Research Information Repository

cortical actin in a living COS-7 cell. The movie is in Supplementary Video 1. Scale bar: 1 μm. (b) Subtraction images of cortical actin. The signals in two consecutive images were subtracted and are shown below. The black filaments indicate new appeared actin filaments, and the white structures indicate the disappeared convergent actin structures in 10 seconds. Scale bar: 1 μm. (c) Elongation of the filament end. Scale bar: 0.5 μm. The arrow indicates the end of the synthesizing filament. (d, e) Effects of cytochalasin B and blebbistatin. (d) AFM images before (left) and after (right) addition of the inhibitor from the same area in the same cell. The images with the addition of inhibitors were started to take within 5 mins after adding the inhibitors to the cell medium. The movies are provided in Supplementary Videos 2 and 3. Scale bar: 1 μm. (e) The rate of end elongation (top left), the density of the filament (top right) and the number of newly appeared actin filaments (bottom) were analyzed from AFM images and summarized. The elongation rate was obtained from >10 filaments, and the density was obtained from 5 independent areas. Error bar indicates SD. *$p < 0.05$ with a two tailed *t*-test.

京都大学 KYOTO UNIVERSITY
A Self-archived copy in
Kyoto University Research Information Repository
https://repository.kulib.kyoto-u.ac.jp
京都大学学術情報リポジトリ KURENAI 紅 Kyoto University Research Information Repository

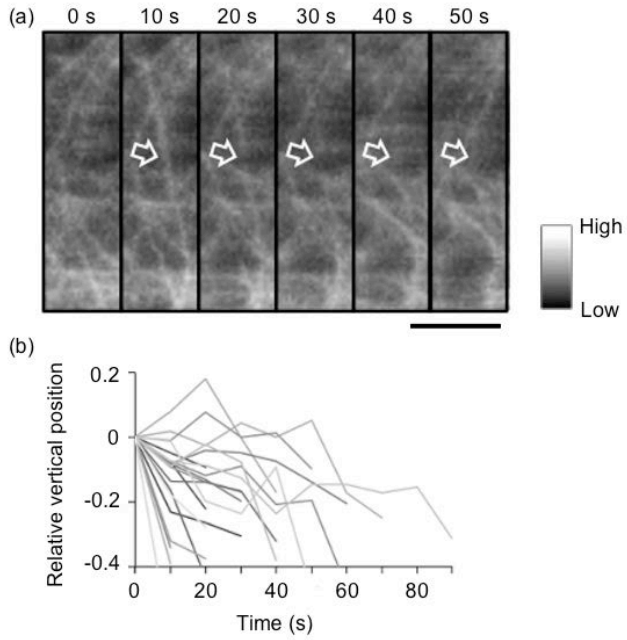

Zhang et al. Fig. 2

Fig. 2. The fate of newly synthesized actin filaments in the cell cortex.

(a) Time series of AFM images. A new filament was synthesized between 0 and 10 s (arrow), and gradually disappeared over time. Scale bar: 0.5 μm. (b) Descension of actin filaments after synthesis. The vertical position of each newly synthesized filament was analyzed and followed over time by section analysis. Twenty individual actin filaments were analyzed. The z-position when the filament appeared (time 0) was set as 0.

京都大学 KYOTO UNIVERSITY
A Self-archived copy in
Kyoto University Research Information Repository
https://repository.kulib.kyoto-u.ac.jp
京都大学学術情報リポジトリ KURENAI 紅 Kyoto University Research Information Repository

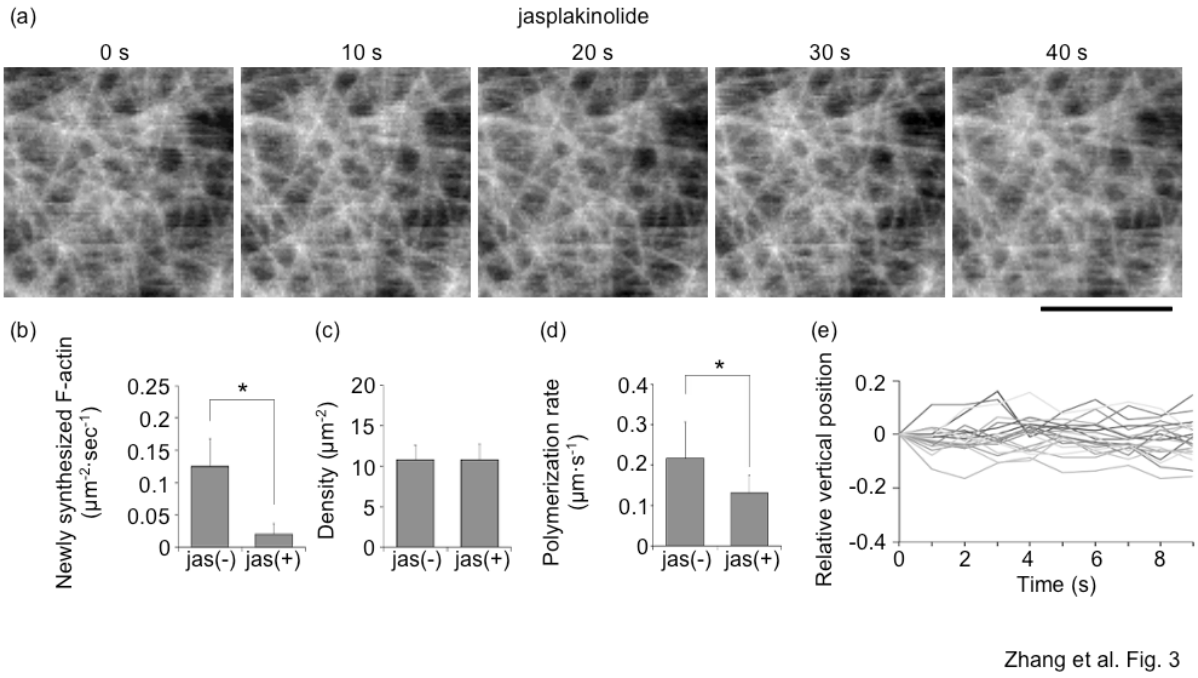

Fig. 3. Effects of jasplakinolide. (a) Time series of AFM images after the addition of 1 μM jasplakinolide. The movie is provided in Supplementary Video 4. Scale bar: 1 μm. (b–d) Statistical analyses of actin dynamics before and after the addition of jasplakinolide. The newly synthesized number (b), density (c), and polymerization rate (d) of actin filaments were measured and summarized. (e) The vertical position of newly-synthesized filament in the presence of jasplakinolide was measured and analyzed as described in Fig. 2. In (b), (c), and (d), data were acquired from at least three different cells. *$p < 0.05$ with a two tailed *t*-test.

京都大学 KYOTO UNIVERSITY
A Self-archived copy in
Kyoto University Research Information Repository
https://repository.kulib.kyoto-u.ac.jp
京都大学学術情報リポジトリ KURENAI 紅 Kyoto University Research Information Repository

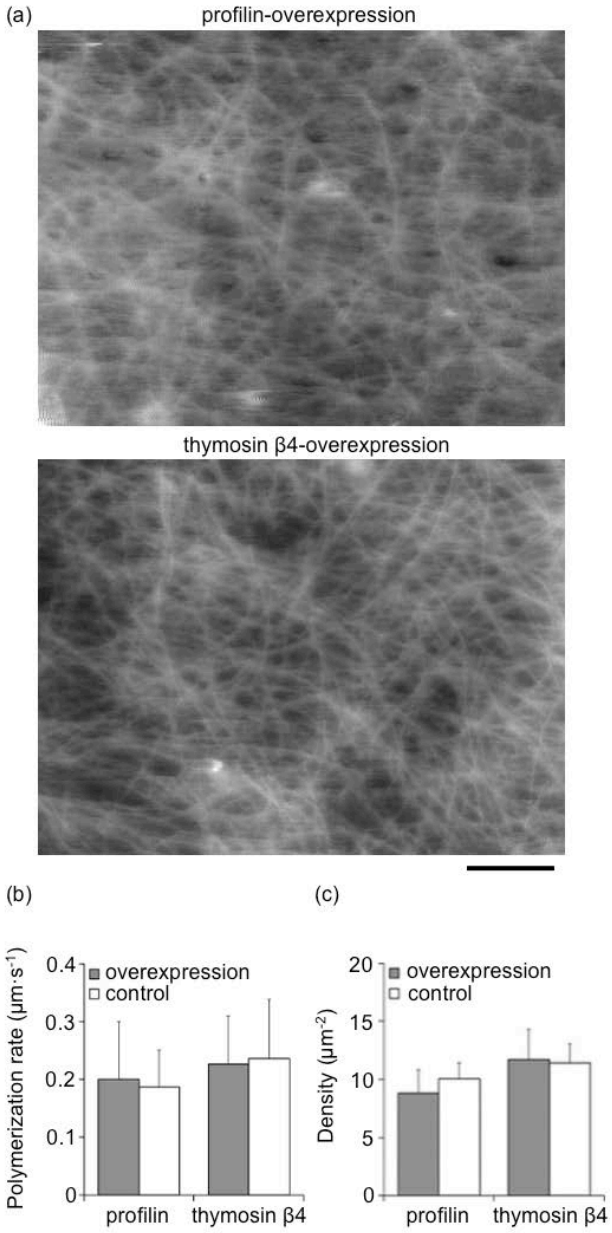

Zhang et al. Fig. 4

Fig. 4. Effects of actin-binding proteins. (a) AFM images of COS-7 cells overexpressing EGFP-profilin (top) or mCherry-thymosin β4 (bottom). Scale bar: 1 μm. The movies are provided in Supplementary Videos 5 and 6. (b, c) Comparison of actin dynamics in control and overexpressing cells. The polymerization rate (b) and filament density (c) were measured from three different cells and summarized.

京都大学 KYOTO UNIVERSITY
A Self-archived copy in
Kyoto University Research Information Repository
https://repository.kulib.kyoto-u.ac.jp
京都大学学術情報リポジトリ KURENAI 紅 Kyoto University Research Information Repository

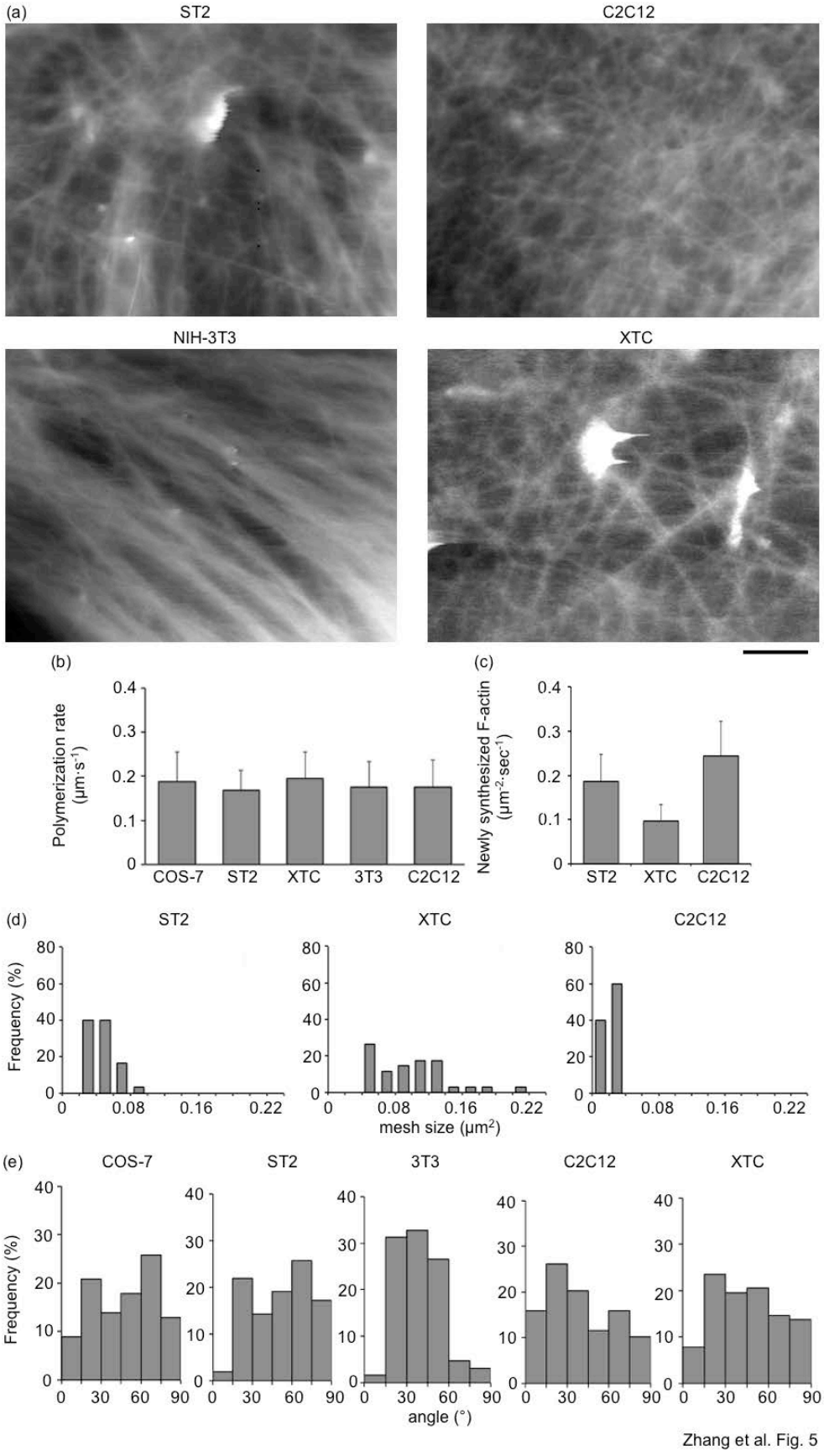

Fig. 5. Actin dynamics in different cell types. （a）AFM images of the cell cortex in ST2,

京都大学 KYOTO UNIVERSITY
A Self-archived copy in
Kyoto University Research Information Repository
https://repository.kulib.kyoto-u.ac.jp
京都大学学術情報リポジトリ KURENAI 紅 Kyoto University Research Information Repository

NIH-3T3, C2C12, and XTC cells. Scale bar: 1 μm. The videos are provided in Supplementary Videos 7–10. (b–e) Comparison of the structure and dynamics of actin filaments. The polymerization rate (b), number of newly synthesized filaments (c), mesh size (d), and the angle of the filament (e) were analyzed and compared. The mesh sizes, the area that is segmented by the actin filaments, were measured from more than 30 regions of each cell type and the angles of the filament, the angle with respect to the horizontal line with the maximal value of 90 degrees, were obtained from more than 60 independent actin filaments in each cell type.

京都大学 KYOTO UNIVERSITY
A Self-archived copy in
Kyoto University Research Information Repository
https://repository.kulib.kyoto-u.ac.jp
京都大学学術情報リポジトリ KURENAI 紅 Kyoto University Research Information Repository

Supplementary Data

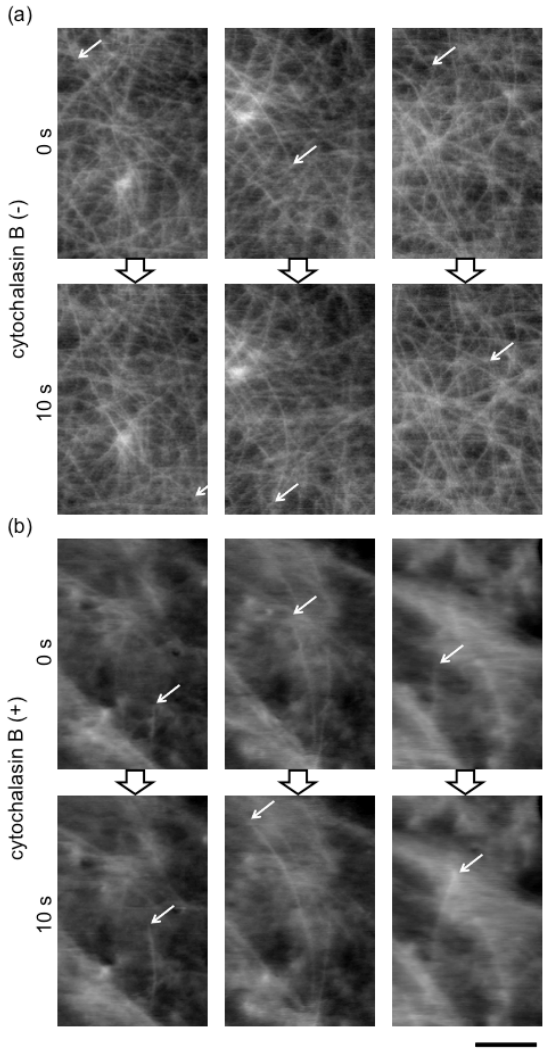

Figure S1. Elongation of the filament end with and without the addition of cytochalasin B. Three typical examples of the elongating filament with (a) and without (b) the addition of cytochalasin B. The elongating filament ends are indicated by arrows. Scale bar: 1 μm.

京都大学 KYOTO UNIVERSITY
A Self-archived copy in
Kyoto University Research Information Repository
https://repository.kulib.kyoto-u.ac.jp
京都大学学術情報リポジトリ KURENAI 紅 Kyoto University Research Information Repository

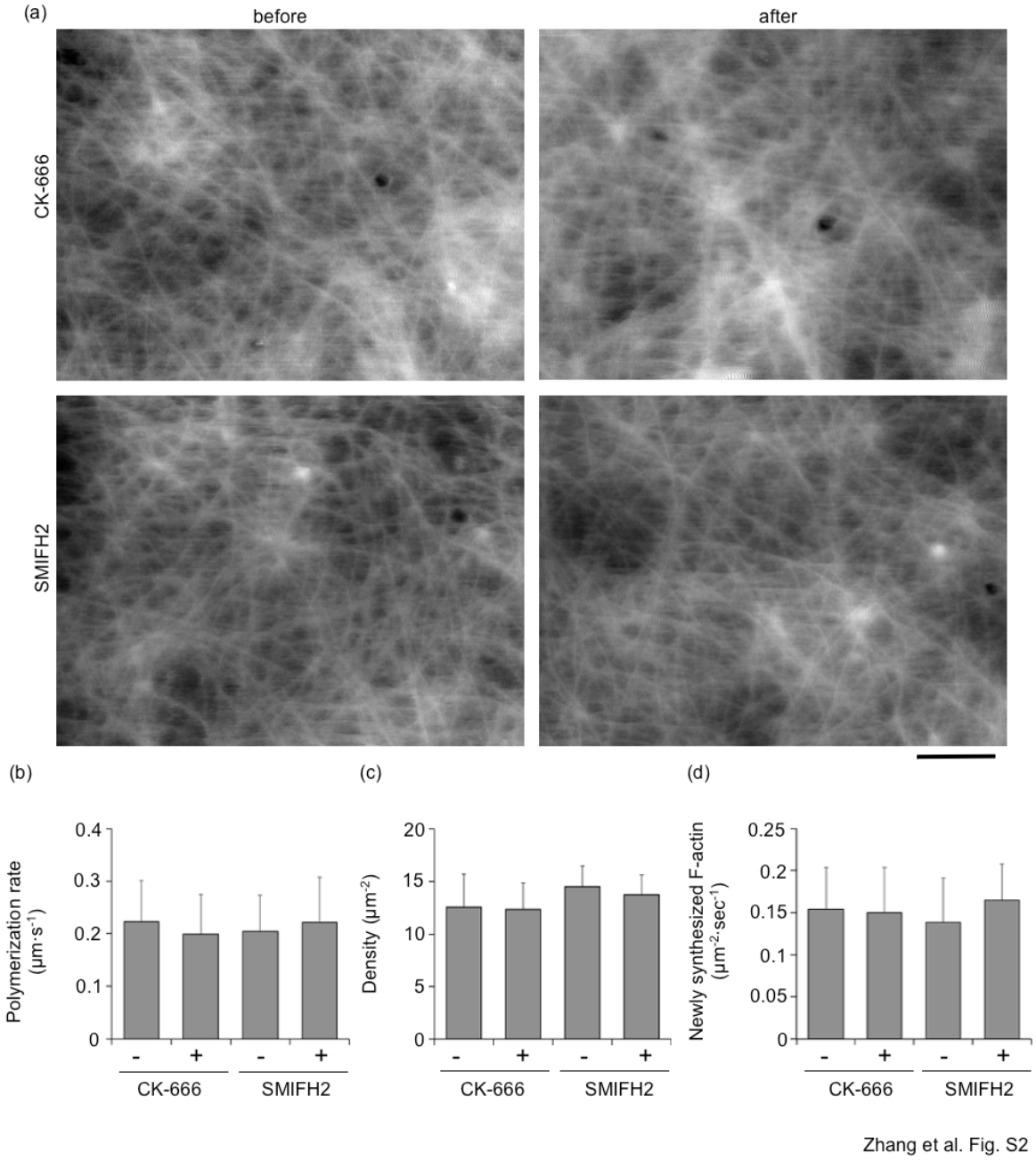

Figure S2. Effects of CK-666 and SMIFH2. (a) AFM images before (left) and after (right) addition of the inhibitors from the same area in the same cell. The images with the addition of inhibitors were started to take within 5 mins after adding the inhibitors to the cell medium. Scale bar: 1 μm. (b–d) Statistical analyses of actin dynamics before and after the addition of CK-666 and SMIFH2. The polymerization rate (b), density (c), and newly synthesized

京都大学 KYOTO UNIVERSITY
A Self-archived copy in
Kyoto University Research Information Repository
https://repository.kulib.kyoto-u.ac.jp
京都大学学術情報リポジトリ KURENAI 紅 Kyoto University Research Information Repository

number (d) of actin filaments were measured and summarized.

Video 1

Time-lapse images of cortical actin layer in a COS-7 cell. Scale bar: 1 μm. Frame rate: 10 sec. The result of image analyses is summarized in Figs. 1 and 2.

Video 2

Effect of cytochalasin B. 2 μM of cytochalasin B was added to the culture medium of COS-7 cell on the microscope stage. Time-lapse imaging was started immediately after the addition of the drug. Scale bar: 1 μm. Frame rate: 10 sec. The result of image analyses is summarized in Fig. 1.

Video 3

Effect of blebbistatin. 50 μM of blebbistatin was added to the culture medium of COS-7 cell on the microscope stage. Time-lapse imaging was started immediately after the addition of the drug. Scale bar: 1 μm. Frame rate: 10 sec. The result of image analyses is summarized in Fig. 1.

Video 4

Effect of Jasplakinolide. 1 μM of Jasplakinolide was added to the culture medium of COS-7 cell on the microscope stage. Time-lapse imaging was started immediately after the addition of the drug. Scale bar: 1 μm. Frame rate: 10 sec. The result of image analyses is summarized in Fig. 3.

京都大学 KYOTO UNIVERSITY
A Self-archived copy in
Kyoto University Research Information Repository
https://repository.kulib.kyoto-u.ac.jp
京都大学学術情報リポジトリ KURENAI 紅 Kyoto University Research Information Repository

Video 5

Overexpression of profilin in COS-7 cell. EGFP-fused profilin was transiently expressed in COS-7 cells. Based on a fluorescence image, the cell with relatively high expression level was chosen and subjected to the AFM imaging. Scale bar: 1 μm. Frame rate: 10 sec. The result of image analyses is summarized in Fig. 4.

Video 6

Overexpression of thymosin β4 in COS-7 cell. mCherry-fused thymosin β4 was transiently expressed in COS-7 cells. Based on a fluorescence image, the cell with relatively high expression level was chosen and subjected to the AFM imaging. Scale bar: 1 μm. Frame rate: 10 sec. The result of image analyses is summarized in Fig. 4.

Video 7

Time-lapse images of cortical actin layer in a NIH-3T3 cell. Scale bar: 1 μm. Frame rate: 10 sec. The result of image analyses is summarized in Fig. 5.

Video 8

Time-lapse images of cortical actin layer in a C2C12 myoblast cell. Scale bar: 1 μm. Frame rate: 10 sec. The result of image analyses is summarized in Fig. 5.

Video 9

Time-lapse images of cortical actin layer in a XTC cell. Scale bar: 1 μm. Frame rate: 10 sec. The result of image analyses is summarized in Fig. 5.

京都大学
KYOTO UNIVERSITY
A Self-archived copy in
Kyoto University Research Information Repository
https://repository.kulib.kyoto-u.ac.jp
京都大学学術情報リポジトリ
KURENAI 紅
Kyoto University Research Information Repository

Video 10

Time-lapse images of cortical actin layer in a ST2 osteoblast cell. Scale bar: 1 μm. Frame rate: 10 sec. The result of image analyses is summarized in Fig. 5.